Efficient aqueous As(III) removal by adsorption on thiol-functionalized mesoporous silica

Amaya Arencibia, María S. López-Gutiérrez, and Jesús M. Arsuaga*

Department of Chemical, Energy and Mechanical Technology,

ESCET, Rey Juan Carlos University.

C/ Tulipán, s/n. 28933-Móstoles, Madrid, Spain

* To whom correspondence should be addressed:

Tel.: +34 91 488 71 47

Fax: +34 91 488 70 68

E-mail address: jesusmaria.arsuaga@urjc.es

This manuscript is intended for the Special Issue **ANQUE-ICCE-CIBIQ 2019**.

Scientifical information of this paper was previously presented at the international meeting **ANQUE-ICCE-CIBIQ 2019 (**Santander, Spain, June 19-21, 2019)

ABSTRACT

BACKGROUND: Arsenic pollution of water supplies is a global problem of environmental concern. Among inorganic species, trivalent arsenite, As(III), is the most toxic and difficult to remove. Conventional treatments usually involve the pre-oxidation to pentavalent arsenic, As(V); however this study is focused on the direct removal of aqueous arsenite species by selective adsorption.

RESULTS: Sulfur-containing adsorbents were prepared from mesostructured SBA-15 silica by functionalization with propylthiol chains. The sulfur content of the synthetized materials, denoted as SBA-15-SH-*x*, reached 4 mmol/g. Kinetics and equilibrium batch experiments showed that all materials were excellent As(III) adsorbents, with maximum capacity as high as 0.46 mmol/g, superior to bibliographic values for comparable materials. pH influence was significant and the best performance occurred at pH = 8. A complementary pelletized material was designed and synthetized to explore the potential use of the adsorbents in the treatment of water streams polluted with arsenic through fixed-bed column experiments. The breakthrough curves obtained in different operative conditions evidenced the viability of the process.

CONCLUSIONS: SBA-15-SH-*x* materials evaluated in this work exhibited very good performance for aqueous As(III) removal by direct adsorption without previous oxidation to As(V). The suitability of the materials was demonstrated through kinetics, equilibrium, and fixed-bed column adsorption experiments.

Keywords: water treatment; arsenic removal; adsorption; SBA-15; thiol functionalization; fixed-bed column

INTRODUCTION

Arsenic pollution of drinking water supplies is an important problem of environmental concern. This metalloid is present in aqueous media due to certain anthropogenic activities, such as mining, wood preservation, or agriculture, and especially through natural processes due to its occurrence in many rocks and sediments as a trace element. Long-term exposure to arsenic can originate several diseases because its high toxicity. The main issue regarding arsenic as a global problem is evidenced by the fact that the presence of this element in drinking water may severely affect more than 100 million people worldwide.[1] Thus, WHO recommended a restrictive drinking water standard with the maximum contaminant level (MCL) fixed at 10 μg/L.[2]

The two most frequent species present in water are the arsenite and arsenate inorganic forms. Trivalent arsenite, As(III), which is more toxic to humans than arsenate, As(V), exhibits higher mobility in the environment and its elimination from water is considered more difficult.[3] Actually, most materials described in the literature for aqueous arsenic removal are more suitable for the removal of As(V);[4,5] hence, a pre-oxidation step is typically prescribed for As(III) solutions. However, pre-oxidation processes usually involve the use of chemical oxidants, high chemical cost, prolonged treatment time, extended operational complexity, and difficulty of implementing adsorption processes on a fixed-bed equipment.[3,6] Therefore, it would be desirable to develop materials to uptake efficiently the arsenite species by direct adsorption.

Many adsorbents were proposed for the removal of arsenic from aqueous solution. Iron oxides/hydroxides, alumina, copper oxides, titania dioxide, zinc oxide, mixed oxides, and carbonaceous materials were studied as materials for arsenic adsorption.[7]

Among other alternatives, inorganic metal oxides such as Fe-Mn oxides,[8] ferrihydrite,[9] and iron oxide in nanoparticles form,[10,11] were recently tested to remove arsenite from

water. Some of these materials exhibited significant adsorption capacities of up to 75 mg/g.[¡Error! Marcador no definido.] Other materials like some specific MOFs, especially when forming composites with Fe_3O_4 or the combination with spinel structures of type $CoFe_2O_4$ with Mil-100(Fe) displayed As(III) adsorption capacities of 100 mg/g and 140 mg/g, respectively.[12] Low cost alternatives, like natural clays that can be modified with chitosan polymers,[13] or pyrolytic carbons obtained from residues, yielded adsorption uptakes smaller, or close, than 1 mmol/g.[14] Mixed binary and ternary oxides, usually containing iron, nickel, cobalt, and/or manganese, as well as their combination with polymers, graphene oxide, carbons or biochar, [15,16,1718,19] were recently reported as effective for arsenite removal with notable retention values, reaching 252.8 mg/g for the mesoporous spinel-type material.[20]

Likewise, thiol-functionalized materials were also proposed as adsorbents for arsenic removal due to the well-known affinity between sulfur and arsenic, The organic groups containing sulfur were observed to interact selectively with As(III), in accordance with the fact that this is the mechanism involved in the arsenic interaction with biomolecules causing toxicity.[21] Therefore, different organic and inorganic materials, such as silica,[22,23,24] polymeric resins,[25] biomass,[26,27] or activated alumina [28,29] were used in the last years as support of mercaptans to develop As(III) selective adsorbents.

Mesostructured silicas can be very suitable for selective adsorption, since they exhibit high surface areas and pore volumes along with uniform mesoporous size.[30] Therefore, many materials of this type were attempted to retain selected target metals by incorporating specific functionalities on the silica walls.[31] Among them, our group developed thiol-functionalized SBA-15 adsorbents for aqueous mercury uptake, achieving suitable textural properties and excellent adsorption performance.[32,33]

Accordingly, these materials could also be a very attractive choice for arsenite removal from water.

In this work, thiol-functionalized materials based on SBA-15 mesoporous silica were evaluated as adsorbents of aqueous arsenite species. It was analyzed the influence on the adsorption performance of the amount of propylthiol groups incorporated by co-condensation into the material structure. The effect of the solution pH on the adsorption process was subsequently studied through equilibrium and kinetics approaches. Finally, fixed-bed column experiments were carried out with agglomerated and pelletized materials to explore the potential application of the adsorbents for the treatment of As(III) polluted water streams.

MATERIALS AND METHODS

Reagents

Tetraethoxysilane [TEOS; $(CH_3CH_2O)_4Si$] and 3-mercaptopropyltrimethoxysilane [MPTMS; $(CH_3O)_3Si(CH_2)_3SH$], used as silica and organic precursors, respectively, and the structure directing agent, Pluronic P123 [triblock poly(ethylene oxide)-poly(propylene oxide)-poly(ethylene oxide), $(PEO_{20}PPO_{70}PEO_{20})$], were purchased from Aldrich. Sodium arsenite, (Na_2AsO, synthesis grade, Fluka) was chosen to prepare the As(III) solutions required for the adsorption experiments. Arsenic standard solution (1.0 g/L in 0.1 mol/L HNO_3 medium, Aldrich) was employed as standard for analysis.

Adsorbents synthesis and characterization

The synthesis of the adsorbents was accomplished by the co-condensation procedure to obtain the propylthiol-functionalized mesoporous SBA-15 silica.[32] Pluronic P123 was dissolved at room temperature in acidic media and heated at 40 ºC. TEOS (37 mmol) was

added to the solution and stirred for 45 min before adding MPTMS organosilane precursor. Different amounts of MPTMS were selected to obtain MPTMS/TEOS molar ratios from 0.1 to 0.4. After stirring (20 h) and aging at 100 ºC (24 h), solid adsorbents were recovered by filtration and drying. The template was removed by ethanol extraction under reflux for 24 h and, after new filtration and drying, the adsorbents were obtained and labeled as SBA-15-SH-*x* with *x* referred to the propylthiol percentage in the structure. Functionalization of pelletized SBA-15 pure silica was also carried out. SBA-15 powder was synthesized following the procedure described above without adding the thiol precursor. After filtering and water washing, the template was eliminated through calcination at 550 ºC for 6 h following a heating rate of 1.8 ºC/min. Then, pellets were prepared by agglomeration of SBA-15 powder with bentonite and methylcellulose (77.5%, 12.5%, and 10%, respectively) with the minimum amount of water necessary to achieve the required consistency.[34] After cooling at 5 ºC for 24 h, the mixture was cylindrically extruded (diameter, 2 mm) and sliced (thickness, 3 mm). Pellets were subsequently calcined under air at low heating rate, a process divided into three stages: 0.2 ºC min^{-1} up to 100 ºC, 0.1 ºC min^{-1} up to 450 ºC, and 0.5 ºC min^{-1} up to 650 ºC, with the intermediate and final temperatures maintained for 1 h, 1 h, and 5 h, respectively. In order to increase the number of silanol groups available on the pellets surface, calcined material was rehydrated by heating the pellets in water at 110 ºC during 24 h. Water excess on the material was then removed by drying under vacuum at 60 ºC for 6 h. After this process, pellets surface was functionalized with propylthiol chains by silylation reaction with MPTMS in toluene reflux. The amount of organic precursor, 9.5 mL for 2 g of agglomerated silica, was selected to provide sulfur content similar to found in the SBA-15-SH-10 material. The resultant solid, recovered by filtration and drying, was labelled as A-SBA-15-SH-10.

Textural characterization of all synthetized materials was accomplished by obtaining the nitrogen adsorption-desorption isotherms at 77 K, after a degasification step in N_2 flow for 8 h at 150 ºC, using a Tristar 3000 Micromeritics equipment. Linearized BET equation was used to determine the BET surface in the 0.05 to 0.20 range of relative pressure. The adsorption branch of the isotherm was selected to estimate the pore size distributions using the B.J.H. model by assuming cylindrical pore geometry. Total pore volume was calculated near the saturation point at a relative pressure around 0.97.[35] Organic sulfur content was thoroughly determined by elemental analysis in a Vario EL III Elementar Analyzer System GMHB.

Arsenite adsorption in batch mode

The isotherms of aqueous arsenite adsorption on all prepared materials, including powder and pellet samples, were determined in the batch mode. To this effect, individual experiments were carried out by stirring 25 mg of the selected solid material in 45 mL of aqueous As(III) solution at 20 ºC during 6 h, the contact time previously observed to ensure equilibrium with the adsorbent powder. Mixtures were filtered shortly afterwards using a syringe filter of 0.22 μm and the final solutions were collected for analysis. However, adsorption experiments accomplished with functionalized pellets were carried out without stirring to prevent fragmentation of the agglomerated and extruded samples and contact time was extended until 12 h. Kinetics experiments were completed in a similar way, although the contact times were picked out within a broad range in this case. Arsenic concentration of the filtered solutions was determined using a NIR/Vis-UV JASCO spectrophotometer, model V-630, by measuring the absorbance at 884 nm after the formation of the molybdate-arsenate complex.[36] Adsorbed arsenic amount was estimated by difference according to Eq. 1:

$$q = \frac{C_0 - C}{m} V \quad (1)$$

where C_0 and C are the arsenic concentrations in the initial and final solutions, q is the adsorbed amount, m is the adsorbent mass, and V is the solution volume.

Fixed-bed column adsorption experiments

Continuous flow experiments were performed across a fixed-bed housed within an upright borosilicate glass cylindrical column (30 cm × 1 cm) packed with pellets of the agglomerated and functionalized A-SBA15-SH-10 material. Pellets were hold between small glass spheres placed in the bottom and top column sections. With this arrangement, the bed length occupied 19.5 cm, corresponding to 5 g of adsorbent The upward flow of the aqueous As(III) solutions through the vertical fixed-bed was achieved by using a peristaltic pump that likewise ensured steady flow rates. The effluent solution was collected at selected time intervals and the arsenic concentration was determined by the same spectrophotometric method referred to above. Prior to the experiments, fixed-bed was conditioned by Milli-Q water circulation for 4 h. Then, Na_2AsO aqueous solutions were flowed through the column at 20 ºC. Arsenic concentration was fixed at 0.05 mol L^{-1} and the natural solution pH, around 8, was measured. Volumetric flow rates ranged from 10 to 160 mL/h.

Breakthrough curves were obtained by plotting the dimensionless concentration C_t/C_0 *vs.* time, where C_t and C_0 are the outlet and inlet adsorbate concentration, respectively. The breakthrough time, t_b, was set for the ratio C_t/C_0 = 0.02 and the exhaust time, t_e, was adopted when the outlet/inlet arsenite concentration ratio reached the value 0.95.

The total amount adsorbed in the column, q_{total} (mg), was calculated from Eq. 2:

$$q_{total} = \frac{Q\,C_0}{1000}\int_0^{t_e}(1-\frac{C}{C_0})\,dt \quad (2)$$

where Q is the flow rate. The total amount of arsenic passing through the column, m_{total} (mg), and the removal percentage were calculated according to Eqs. 3 and 4:

$$m_{total} = \frac{C_0\,Q\,t_e}{1000} \quad (3)$$

$$R(\%) = \frac{q_{total}}{m_{total}} \times 100 \quad (4)$$

RESULTS AND DISCUSSION

Physicochemical properties of SBA-15-SH-*x* adsorbents

The complete characterization of all synthetized thiol-functionalized SBA-15 adsorbents in powder form was previously reported, including TEM and SEM images, small angle XRD difractograms, ^{29}Si MAS-NMR analysis, and FTIR spectroscopy. Likewise, chemical and thermal stability was widely verified.[33] Therefore, only some relevant textural properties and the sulfur content of the samples were discussed here, mainly for comparison with the new pelletized materials. The nitrogen adsorption-desorption isotherms at 77 K corresponding to the powder-like materials belonged to IUPAC type IV,[35] illustrating their mesoporous condition, although the adsorbed nitrogen volume thoroughly declined when increasing the organic amount incorporated to the SBA-15 pure silica. Accordingly, the pore diameter, specific surface area, and pore volume of the materials systematically diminished from SBA-15-SH-10 to SBA-15-SH-40, as can be observed in Table 1 that summarized the textural properties and sulfur content for all adsorbents prepared in this work.

Regarding the pelletized material A-SBA-15-SH-10, N_2 sorption isotherm could be classified as intermediate between IUPAC types IV and V, as shown in Fig. 1a, with a striking reduction of porosity in comparison with SBA-15-SH-10 powder. Since the agglomeration process with bentonite and methylcellulose to produce A-SBA-15 significantly reduced the surface area and pore volume, but preserved the mesostructure, it should be presumed that the most important degradation of the structure occurred in the course of the thiol-functionalization process, probably due to pore collapse, as exhibited in Fig. 1b.

Aqueous arsenite adsorption on SBA-15-SH-*x* materials

The experimental isotherms of As(III) adsorption on the SBA-15-SH-*x* materials were obtained at 20 ºC up to saturation to determine the maximum adsorption capacities and the affinity between the arsenite species and thiol active sites. Figure 2 displayed the experimental isotherms that belonged to type I or type L, according to the IUPAC[35] or Giles' classifications[37], respectively. The isotherms showed a sharp increase of the As(III) retention at low concentration and a steady achievement of the adsorbent saturation, associated with the monolayer formation of arsenite species on the material surface through chemisorption. It is patent from Fig. 2 that both the maximum As(III) adsorption capacity of each material and the initial slope of the isotherms were clearly related to the degree of thiol functionalization, thoroughly increasing from SBA-15-SH-10 to SBA-15-SH-40.

In order to outline the specific behavior of every adsorbent, experimental data were compared to the fits provided by the Langmuir and Freundlich isotherms. The Langmuir model explains the adsorption on homogeneous surfaces assuming the same affinity of the adsorbate for all active sites with complete surface coverage to form a monolayer at

high equilibrium concentrations of sorbate in solution (C_e). Freundlich isotherm describes adsorption on heterogeneous surfaces as well as multilayer sorption. Both models are expressed by the following mathematical expressions:

Langmuir $$q_e = \frac{Q_0\, b\, C_e}{1 + b\, C_e} \quad (5)$$

Freundlich $$q_e = K_F\, C_e^{1/n} \quad (6)$$

where Q_0 is the maximum adsorption capacity, *i.e.* the adsorbate amount needed to complete a monolayer, and b is the Langmuir constant related to the intensity of the interaction adsorbent/adsorbate. K_F, and n, are the empirical constants of Freundlich equation, which are associated to the adsorption capacity and the adsorption energy, respectively.

Table 2 showed the results of the mathematical fitting provided by the Langmuir and Freundlich models. As presumed after glancing at the isotherms shape, the adsorption behavior was much better described by the Langmuir equation that yielded regression coefficients, R^2, higher than 0.99. Therefore, non-linear fitting to Langmuir model was included as solid curves in Fig. 2 showing good agreement to experimental values. Hence, it was concluded that As(III) adsorption on SBA-15-SH-*x* materials involved the formation of a superficial monolayer through chemisorption between thiol active groups and arsenic species.

It is worth emphasizing the significant arsenic adsorption capacities measured for the SBA-15-SH-*x* materials, especially when the amount of thiol groups was increased. As read in Table 2, maximum adsorption capacity achieved values as high as 0.46 mmol/g for the SBA-15-SH-40 sample. This quantity was very remarkable, taking into account other results found in literature for analogous materials. For instance, thiol-functionalized

materials prepared from activated alumina were reported to adsorb 0.15 mmol As(III)/g.[29] Regarding mesostructured materials, the adsorption capacity observed in this work was considerably higher than the previously reported for mercaptopropylthiol functionalized HMS silica (0.25 mmol As(III)/g), despite this last value was obtained with a material highly functionalized that incorporated up to 50% of mercaptopropyl groups.[24] Therefore, the SBA-15-SH-*x* adsorbents appeared as good arsenite adsorbents, probably due to their open structure that allowed As(III) to diffuse and easily access to the binding sites. Moreover, since the adsorption affinity was significantly high, as revealed by the steep initial slope of the isotherms, the efficacy of the adsorbents at low concentration should be adequate to reduce the arsenite species traces below the values established by water regulation.

Regarding the mechanism of the adsorption process, it was proposed by several authors that inorganic arsenite anchoring to the adsorbent surface would involve the formation of arsenic/sulfur complexes, where every As(III) species was bound to three thiol groups according to Scheme 1,[38] as also occurred in arsenic trisulfide, the main inorganic compound of arsenic.

The sulfur to arsenic molar ratio at saturation of the materials was also included in Table 2. As seen, the value determined for SBA-15-SH-10 was reasonably in agreement with the expected 3:1 ratio; however, a regular increase from 4.4 to 8.6 was observed as the thiol functionalization enlarged from 10% to 40%. Thus, the maximum arsenic adsorption capacity did not enhance linearly with thiol functionalization and more sulfur atoms were increasingly needed for each retained arsenite species. This fact could be probably related to the accessibility of arsenite species towards the thiol groups.

Influence of pH on arsenite adsorption

The initial pH of the As(III) solutions used in the experiments described in the precedent section was the natural for the studied arsenite concentration, *i.e.* nearly pH = 8. It is worth mentioning that the resultant pH after adsorption was lower. However, medium pH is one of the most important variables affecting the adsorption process, since determines the predominant species of the adsorbate in the solution and simultaneously influences the surface of the adsorbent and the nature of its active sites. Thus, the pH effect was also investigated from both kinetics and equilibrium approaches. The material SBA15-SH-40 was selected due to its higher arsenic adsorption capacity. The initial pH of the arsenite solutions was shifted between 2 and 12 by adding nitric acid or sodium hydroxide, respectively. It was previously reported that the synthetized materials SBA-15-SH*x* were chemically very stable at acidic, neutral and mild basic media.[32] Conversely, some degradation of the mesoporous silica structure could be expected at the more basic pH; however, the temporal evolution of the adsorption capacity of the material at basic pH showed no evident decay for the first six hours.

Regarding adsorption equilibrium, the experimental isotherms were plotted in Fig. 3 with the best Langmuir's fits shown as solid curves. Table 3 listed the calculated Q_0 parameters estimated from the Langmuir model and the experimental maximum capacities, denoted as q_e(max). An excellent agreement was found for each tested pH value, as read in Table 3. It was concluded from Fig. 3 and Table 3 that the adsorption capacity of the material SBA-15-SH-40 steadily increased with solution pH up to a maximum that matched the natural of the aqueous $NaAsO_2$ solutions (pH ≈ 8). When pH exceeded this value, the adsorption capacity significantly diminished, since the maximum adsorption capacity observed at the natural pH was 0.46 mmol/g, whereas for pH = 12 this value decreased to 0.27 mmol/g, *i.e.* a reduction higher than 40%. To explain this behavior, it should be considered the different arsenic species present in the medium. Fig. 4 showed the

speciation diagram for a 50 mg/L As(III) solution as a pH function. Arsenious acid, H_3AsO_3, was the main species up to pH = 9.2, although the occurrence of the monovalent anion $H_2AsO_3^-$ was visible in the medium from pH = 7, being predominant in the range 9.2 - 12.1.[39] Divalent anion $HAsO_3^{2-}$ appeared from pH = 10, but was important only beyond the scope of this work, from pH 12.1 to 13.5, while the presence of the trivalent anion, AsO_3^{3-} was irrelevant, except for the highest pH values, over 13. Regarding the behavior of the adsorbent surface, the pK_a of the thiol active groups was expected to lie between 10 and 11.[40] Therefore, taking into account all these facts and the values reported in Table 3, it was concluded that the strongest affinity between the SBA-15-SH-40 adsorbent and the several aqueous As(III) species must be ascribed to the H_3AsO_3 compound. The significant adsorption reduction found at higher pH values was attributed to the increasing electrostatic repulsion between the anionic As(III) species present in the aqueous solution and the negatively charged surface of the silica adsorbent. The minor adsorption decline also observed below neutral pH could be related to the more difficult deprotonation of the thiol group in acidic medium, a preliminary step required to the formation of the sulfur-arsenic bonds. A similar effect was previously observed for other adsorption processes on thiol groups.[32]

The pH influence on the adsorption process was likewise studied through kinetics experiments accomplished with the same adsorbent, SBA-15-SH-40, and aqueous As(III) solutions with arsenic initial concentration of 50 mg/L. The pH effect was examined at the values 2, 5, 8, 10, and 12. Figure 5 showed the adsorbed As(III) amount as a function of the contact time at the different pH values. In all cases, the adsorption equilibrium was attained for a time around 300 min, regardless of solution pH. Three semi-empirical models were tested to analyse the overall kinetics, namely pseudo-first order, pseudo-second order, and Elovich models.[41] Neither the pseudo-first order model nor the Elovich

equation were suitable to fit the experimental curves. Conversely, the kinetics profiles for aqueous As(III) adsorption on the SBA-15-SH-40 sample were adequately described by the pseudo-second-order mathematical model (Eq. 7), that was used after integration from $t = 0$ and $q_t = 0$ to yield the lineal form (Eq. 8).

$$\frac{dq_t}{dt} = k_2 \left(q_e - q_t\right)^2 \qquad (7)$$

$$\frac{t}{q_t} = \frac{1}{k_2 \, q_e^{\,2}} + \frac{t}{q_e} \qquad (8)$$

The fittings were successful in every case (solid curves in Fig. 5), showing regression coefficients of the fits, R^2, higher than 0.98. The related parameters k_2 and q_e were summarized in Table 4. Concerning pH dependence, conclusions were similar to the extracted from the equilibrium study. As can be seen in Fig. 5, the most favorable pH for adsorption was the natural pH of the arsenite solution with minor reduction in acidic medium and significant decline at higher pH values. Nevertheless, it is worth mentioning that kinetics curves exhibited no apparent anomalies at the most basic pH.

Fixed-bed arsenite adsorption

The adsorption capacity of the pellets prepared to fill the column was checked under equilibrium conditions prior to the fixed-bed experiments. As displayed in Fig. 2, the adsorption isotherm corresponding to the A-SBA-15-SH-10 sample was also classified as IUPAC type I, *i.e.* with a high affinity for As(III) species at low concentration. However, its maximum arsenic adsorption capacity (0.21 mmol g^{-1}) exhibited an apparent reduction in comparison with the material powder obtained by the co-condensation method with similar sulfur content, SBA-15-SH-10 (0.27 mmol g^{-1}). This diminution was attributed to the observed porosity decrease combined with the loss of accessibility to all the thiol groups incorporated to the pellets.

Different column dynamics adsorption experiments were carried out to test the performance of the pelletized material used as fixed-bed by modifying the flow rate of the arsenic feed solution from 10 to 160 mL h^{-1}.[42] The breakthrough curves obtained for the As(III) capture were displayed in Figure 6a and the estimated parameters extracted from the curves were listed in Table 5.

As expected, the breakthrough and exhaust times deeply depended on the flow rate; in addition, the well-shaped breakthrough curves exhibited steeper profiles at earlier times when flow rate increased. For instance, the breakthrough time extended from 182 min to 3135 min, while the flow rate reduced from 160 mL h^{-1} to 10 mL h^{-1}. At the lowest value, the residence time significantly improved, thus facilitating the accessibility of the arsenic species to the thiol specific sites of the adsorbent particles. However, the arsenic retention total capacity showed a rather moderate dependence on the flow rate. Accordingly, the removal percentage for the lowest flow rate revealed a notable yield (92%), calculated with Eq. 4 from the total uptake and the feed amount of As(III). When the flow rate increased to 80 and 160 mL h^{-1}, the removal percentage reduced to nearly 88% and 82%, respectively. Consequently, the experiments carried out with a simple fixed-bed column evidenced the potentiality of materials similar to A-SBA-15-SH-10 for practical use in the treatment of water streams containing As(III) species.

To complete the arsenic adsorption study, it was evaluated the possible competence with other adsorbates present in the medium. Therefore, the fixed-bed column packed with pellets of the agglomerated adsorbent A-SBA-15-SH-10 was also tested for the treatment of continuous water streams containing mixtures of As(III) and Hg(II) species, due to the probed outstanding affinity of thiol-functionalized silica with mercury compounds.[32,33] To this effect, aqueous Hg(II) solutions were prepared from $HgCl_2$ and mercury concentration was determined by means of CV-AFS, as described elsewhere.[42] Fig. 6b

displayed four breakthrough curves corresponding to pure arsenic solution, pure mercury solution, and equimolar mixtures of both elements. The concentration of the solution feed and the flow rate were fixed at 0.05 mmol L^{-1} for each element and 80 mL h^{-1}, respectively. It was apparent that the breakthrough times for mercury solutions were widely larger than the observed with arsenic solutions due to the well-known strong liking of the thiol groups for mercury species and the more favorable 1:1 mercury/sulfur stoichiometry against the 1:3 arsenic/sulfur stoichiometry. Furthermore, the breakthrough and exhaust times decreased for both species when the experiments were carried out with the mixture, although the As(III) breakthrough curve was most affected, as glancing at Fig. 6b. Nevertheless, despite the degradation of the performance of the fixed-bed column for arsenic retention observed in the presence of mercury species, it should be concluded that adsorption capacity of the thiol-functionalized SBA-15 materials, both in batch and continuous experiments, was very adequate for arsenite removal.

CONCLUSIONS

All thiol-functionalized SBA-15 silicas prepared in this study through a one-step synthesis by the co-condensation method have been probed very effective adsorbents for arsenite removal from aqueous solution. The As(III) adsorption isotherms has been completed up to saturation by means of batch experiments for all materials powder, denoted as SBA-15-SH-*x*, and it has been confirmed the ability of the Langmuir model to fit them. The observed high affinity of the adsorbents with aqueous As(III) at low concentration shows the feasibility of reducing arsenic levels in solution below the regulated limit. Maximum arsenic adsorption capacity increases with the thiol functionalization degree, reaching values as high as 0.46 mmol/g, an amount clearly superior to found in the literature for comparable materials. The solution pH plays a

significant role in the arsenite adsorption on the SBA-15-SH-*x* materials as evidenced through kinetics and equilibrium experiments. The best performance occurs at pH = 8, the natural of the studied arsenite solutions, being more marked the loss of efficacy for very alkaline pH. Finally, in order to explore the practical use of the materials for the treatment of water streams polluted with arsenite, it has been developed a new adsorbent agglomerated with a bentonite and methylcellulose (A-SBA-15-SH-10). The fixed-bed experiments carry out using a vertical column with bottom-up flow have shown the satisfactory performance of the material in different operating conditions, even in the presence of mercury, a strong rival for the active sites of the adsorbent.

ACKNOWLEDGMENTS

Authors thank the Spanish Ministry of Economy and Competitiveness (MINECO) for the support through the research projects CTM2012-34988 and CTM2015-69246-R. The Regional Government of Madrid is also acknowledged by its contribution through Project S2013/MAE-2716-REMTAVARES-CM.

REFERENCES

1 Amini M, Abbaspour C, Berg M, Winkel L, Hug SJ, Hoehn E, Yang H and Johnson CA, Statistical Modeling of Global Geogenic Arsenic Contamination in Groundwater. *Environ. Sci. Technol.* **42**:3669-3675 (2008).

2 Arsenic in drinking water. WHO Guidelines for Drinking-water Quality https://www.who.int/water_sanitation_health/dwq/chemicals/arsenic.pdf

3 Singh R, Singh S, Parihar, P, Singh VP and Prasad SM. Arsenic contamination, consequences and remediation techniques: A review. *Ecotox. Environ. Safety* **112**:247-270 (2015).

4 Hao L, Liu M, Wang N and Li G, A critical review on arsenic removal from water using iron-based adsorbents, *RSC Advances* **69**:39545-39560 (2018).

5 Mostafa MG and Hoinkis J, Nanoparticle adsorbents for arsenic removal from drinking water: a review. *Int. J. Environ. Sci. Management Engineer. Res.* **1**:20-31 (2012).

6 Bissen M and Frimmel FH, Arsenic — a Review. Part II: Oxidation of Arsenic and its Removal in Water Treatment, *Acta Hydrochim Hydrobiol.*, **31**:97–107 (2003).

7 Lata S and Samadder SR, Removal of arsenic from water using nano adsorbents and challenges: A review, *J. Environ. Manage.*, **166:**387-406 (2016).

8 Szlachta M, Gerda V and Chubar N, Adsorption of arsenite and selenite using an inorganic ion exchanger based on Fe-Mn hydrous oxide, *J. Colloid Interf. Sci.*, **365**:213-221 (2012).

9 Hoffmann M., Mikutta C and Kretzschmar R. Arsenite binding to sulfhydryl groups in the absence and presence of ferrihydrite: A model study, *Environ. Sci. Technol.*, **48**:3822-3831 (2014).

10 Sahu, UK, Sahu, MK, Mahapatra, SS and Patel R.K. Removal of As(III) from Aqueous Solution Using Fe_3O_4 Nanoparticles: Process Modeling and Optimization Using Statistical Design, *Water, Air, and Soil Pollution* **228:**1-5 (2017).

11 Ramos-Guivar JA, Bustamante DA, Gonzalez, JC, Sanches EA, Morales MA, Raez, JM, López-Muñoz, M-J and Arencibia A. Adsorption of arsenite and arsenate by binary and ternary magnetic nanocomposites with high iron oxide content. *Appl. Surf. Sci.*, **454**:87-100 (2018).

12 Wang C, Luan J and Wu C, Metal-organic frameworks for aquatic arsenic removal. *Water Research,* 158: 370-382 (2019)

13 Saleh T, Sarı A and Mustafa Tuzen M, Chitosan-modified vermiculite for As(III) adsorption from aqueous solution: Equilibrium, thermodynamic and kinetic studies, *J. Mol. Liq.*, **219**:937-945 (2016).

14 Mouzourakis E, Georgiou Y, Louloudi M, Konstantinou I and Deligiannakis Y. Recycled-tire pyrolytic carbon made functional: A high-arsenite [As(III)] uptake material PyrC350®. *J. Hazard. Mater.*, 326:177-186 (2017)

15 Zhang, G, Luo, J, Wang L. Polyvinyl alcohol-stabilized granular Fe–Mn binary oxide as an effective adsorbent for simultaneous removal of arsenate and arsenite, *Environ. Technol.*, doi10.1080/09593330.2019.1575479 (2019).

16 Mohd A, Pei N, Ahmad SG and Ismail F. Highly adsorptive polysulfone/hydrous iron-nickel-manganese (PSF/HINM) nanocomposite hollow fiber membrane for synergistic arsenic removal. *Sep. Purif. Technol.* 213:162-175 (2019)

17 Majia S, Ghosh A, Gupta K, Ghosh A, Ghorai U, Santra A, Sasikumar P, Ghosh UC, Efficiency evaluation of arsenic(III) adsorption of novel graphene oxide@iron-aluminium oxide composite for the contaminated water purification, *Sep. Purif. Technol.*, **197**:388-400 (2018)

18 Ghosh A, Biswas S, Sikdar S and Saha R. Morphology Controlled Fabrication of Highly Permeable Carbon Coated Rod-Shaped Magnesium Oxide as a Sustainable Arsenite Adsorbent, *Ind. Engin. Chem. Res.*, 58:10352-10363 (2019).

19 Kim J, Song J, Lee SM and Jung J, Application of iron-modified biochar for arsenite removal and toxicity reduction, *J. Ind. Engin. Chem.*, **80**:17-22 (2019).

20 Georgiou Y, Papadas IT, Mouzourakis E, Skliri E, Armatas GS, Deligiannaki Y, Mesoporous spinel $CoFe_2O_4$ as an efficient adsorbent for arsenite removal from water: High efficiency: Via control of the particle assemblage configuration, *Environ. Sci: Nano.* **6**: 1156-1167 (2019),

21 Rey NA, Howarth EC and Pereira-Maia EC, Equilibrium characterization of the As(III)-cysteine and the As(III)-glutathione systems in aqueous solution. *J. Inorg. Biochem.*, **98**:1151-1159 (2004).

22 Howard AG, Volkan M and Ataman DY, Selective pre-concentration of arsenite on mercapto-modified silica gel, *Analyst* **112**: 159–162 (1987).

23 Bennett WW, Teasdale PR, Panther JG, Welsh, DT, and Jolley DF. Speciation of dissolved inorganic arsenic by diffusive gradients in thin films: Selective binding of As III by 3-mercaptopropyl-functionalized silica gel, *Anal. Chem.* **83**:8293-8299 (2011).

24 McKimmy E, Dulebohn J, Shah J and Pinnavaia TJ, Trapping of arsenite by mercaptopropyl-functionalized mesostructured silica with a wormhole framework. *Chem. Commun*. 3697–3699 (2005).

25 Dominguez L, Yue ZR, Economy J and Mangun CL. Design of polyvinyl alcohol mercaptyl fibers for arsenite chelation, *React. Funct. Polym.* **53**:205–215(2002).

26 Teixeira MC and Ciminelli VST, Development of a biosorbent for arsenite: structural modeling based on X-ray spectroscopy, *Environ. Sci. Technol*. **39**:895–900 (2005).

27 Yang R, Su Y, Aubrech KB, Wang X, Ma H, Grubbs RB, Hsiao BS and Chu B, Thiol-functionalized chitin nanofibers for As(III) adsorption, *Polymer* **60**:9-17 (2015).

28 Hao J, Han M-J and Meng X, Preparation and evaluation of thiol-functionalized activated alumina for arsenite removal from water, *J. Hazard. Mater.* **167**:1215–1221 (2009).

29 Hao J, Han M-J, Wang C and Meng X, Enhanced removal of arsenite from water by a mesoporous hybrid material –Thiol-functionalized silica coated activated alumina, *Micropor. Mesopor. Mater.*, **124**:1-7 (2009).

30 Whang Y and Zhao D. On the controllable soft-templating approach to mesoporous silicates. *Chem. Rev.* **107**:2821-2860 (2007).

31 Diagboya PNE and Dikio ED, Silica-based mesoporous materials; emerging designer adsorbents for aqueous pollutants removal and water treatment, *Micropor. Mesopor. Mater.* **266**: 252-267 (2018).

32 Aguado J, Arsuaga JM and Arencibia A. Adsorption of aqueous mercury(II) on propylthiol-functionalized mesoporous silica obtained by co-condensation. *Ind. Eng. Chem. Res.* **44**: 365-371 (2005).

33 Aguado J, Arsuaga JM and Arencibia A. Influence of synthesis conditions on mercury adsorption capacity of propylthiol functionalized by co-condensation *Micropor. Mesopor. Mater.* **109**: 513-524 (2008).

34 Martınez F, Melero, J Botas JA, Pariente MI, and Molina R. Treatment of Phenolic Effluents by Catalytic Wet Hydrogen Peroxide Oxidation over Fe_2O_3/SBA-15 Extruded Catalyst in a Fixed-Bed Reactor, *Ind. Eng. Chem. Res.* **46**: 4396-4405 (2007).

35 Thommes M, Kaneko K, Neimark AV, Olivier JP, Rodriguez-Reinoso F, Rouquerol J and Kenneth S.W. Sing. Physisorption of gases, with special reference to the

evaluation of surface area and pore size distribution (IUPAC Technical Report). *Pure Appl. Chem.* (2015).

36 López-Muñoz, M. J.; Revilla, A.; Alcalde, G, Brookite TiO_2-based materials: Synthesis and photocatalytic performance in oxidation of methyl orange and As(III) in aqueous suspensions *Catal. Today*, **240**:138-145 (2015).

37 Giles, C.H., Smith, D. and Huitson, A. A General Treatment and Classification of the Solute Adsorption Isotherm. I. Theoretical. *J. Colloid. Interf. Sci.* 47:755-765 (1974).

38 Anne M. Spuches; Harriet G. Kruszyna; Anne M. Rich; Dean E. Wilcox, Thermodynamics of the As(III)−Thiol Interaction: Arsenite and Monomethylarsenite Complexes with Glutathione, Dihydrolipoic Acid, and Other Thiol Ligands, *Inorg. Chem.* **44**:2964-2972 (2005).

39 Howe KJ, Hand DW, Crittenden JC, Trussell R and Tchobanoglous G. Principles of water treatment. Canadá. MWH. ISBN: 9780470405383 (2012).

40 Danehy JP and Parameswaran KN. Acidic Dissociation Constants of Thiols. *J. Chem. Eng. Data* **13**:386−389 (1968).

41 Y.S. Ho YS, and McKay G. Application of Kinetic Models to the Sorption of Copper (II) on to Peat. *Adsorption Sci. Technol.* **20**:797-815 (2002).

42 Arsuaga JM, Aguado J, Arencibia A, and López-Gutiérrez M.S. Aqueous mercury adsorption in a fixed bed column of thiol functionalized mesoporous silica. *Adsorption* **20**:311-319 (2014).

Table 1. Textural properties and sulfur content of powder-like and pelletized materials.

Material	D_p (nm)	S_{BET} (m^2/g)	V_p (cm^3/g)	S content (mmol/g)
SBA-15	6.9	710	0.83	–
SBA-15-SH-10	6.3	680	0.79	1.20
SBA-15-SH-20	5.1	346	0.47	1.99
SBA-15-SH-30	4.6	259	0.29	2.98
SBA-15-SH-40	4.4	145	0.19	3.97
A-SBA-15	6.9	318	0.67	–
A-SBA-15-SH-10	–	156	0.15	1.21

Table 2. Estimated parameters from Langmuir and Freundlich fits to the experimental As(III) adsorption isotherms on SBA-15-SH-*x* materials at 20 ºC.

	Langmuir model			Freundlich model			
Adsorbent	Q_0 (mmol/g)	b (L/mg)	R^2	n	K_F *(mmol/g)(L/mg)*	R^2	Molar ratio sulfur/As(III)
SBA15-SH10	0.27	0.33	0.990	1.61	0.027	0.811	4.4
SBA15-SH20	0.32	0.38	0.999	5.59	0.014	0.968	6.2
SBA15-SH30	0.39	0.39	0.998	7.29	4.798	0.977	7.6
SBA15-SH40	0.46	0.41	0.999	0.27	0.266	0.917	8.6

Table 3. Experimental maximum capacities, $q_e(max)$, obtained for the adsorption of As(III) on SBA-15-SH-40 and estimated Q_0 parameters from the Langmuir model.

pH	2	5	8	10	12
$q_e(max)$/(mmol/g)	0.35	0.39	0.46	0.30	0.26
Q_0/(mmol/g)	0.34	0.37	0.46	0.29	0.26

Table 4. Estimated parameters for the fitting of pseudo-second order kinetic model to experimental kinetic results

pH	2	5	8	10	12
q_e/(mmol/g)	0.39	0.43	0.48	0.30	0.26
k_2 /(g/min·mmol)	0.032	0.031	0.037	0.066	0.099

Table 5. Dynamic parameters estimated from breakthrough curves for As(III) adsorption on fixed-bed column experiments.

Q (mL h^{-1})	t_b (min)	t_e (min)	As(III) removal (%)
10	3135	3870	91.9
80	363	480	88.6
160	182	277	82.5

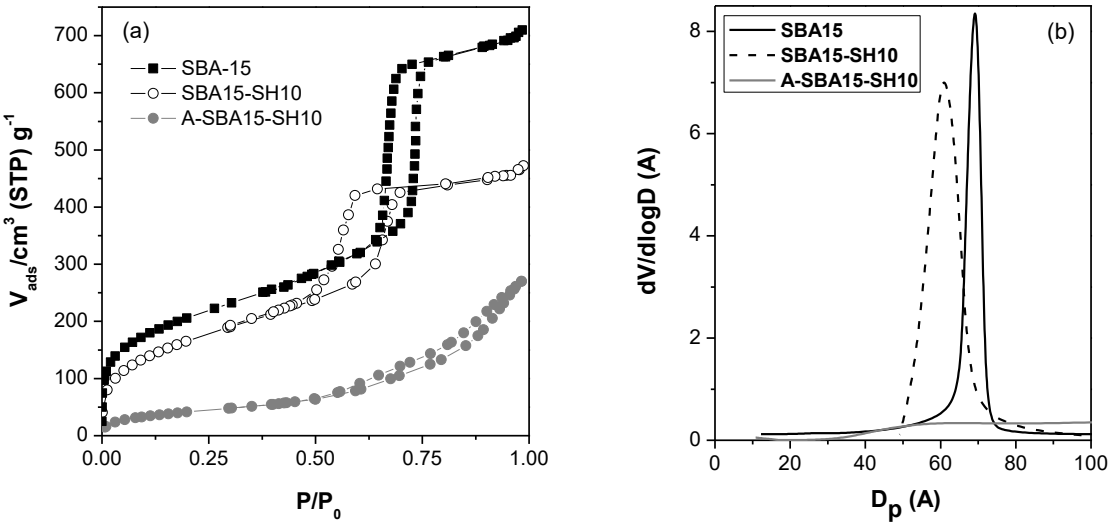

Figure 1. Textural properties of powder-like SBA-15 and SBA-15-SH-10, and agglomerated A-SBA15-SH-10 solid. (a) Nitrogen adsorption-desorption isotherms at 77 K. (b) B.J.H. pore size distributions.

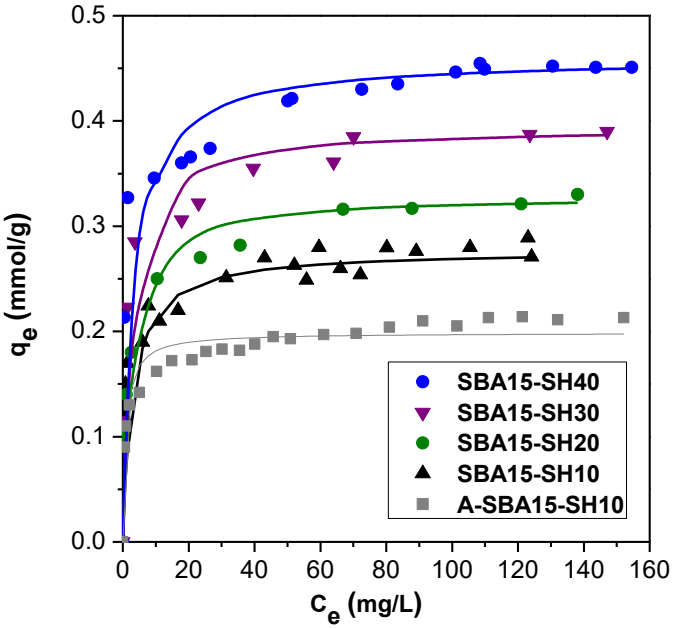

Figure 2. Aqueous arsenite adsorption isotherms at 20 ºC and initial pH = 8 for SBA-15-SH-*x* powder and agglomerated A-SBA-15-SH-10 materials. Solid curves obtained from Langmuir's fitting.

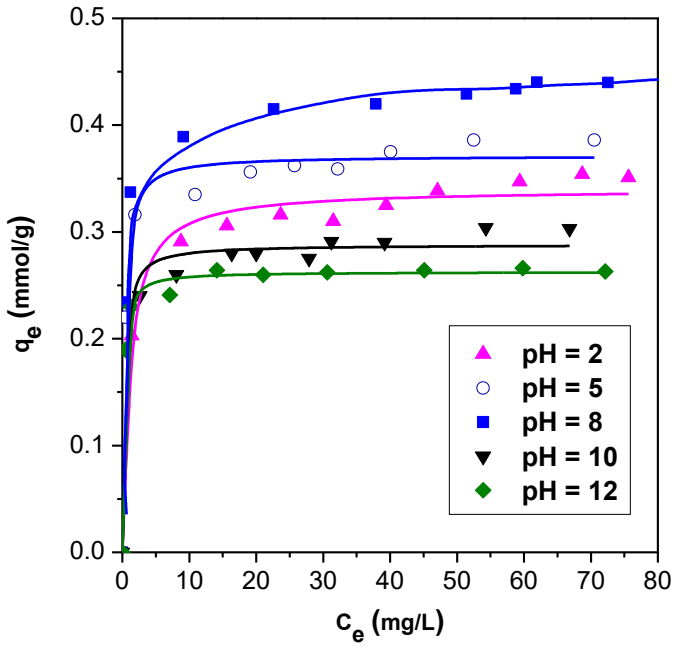

Figure 3. pH dependence of aqueous arsenite adsorption isotherms at 20 ºC for SBA-15-SH-40. Solid curves obtained from Langmuir's fitting.

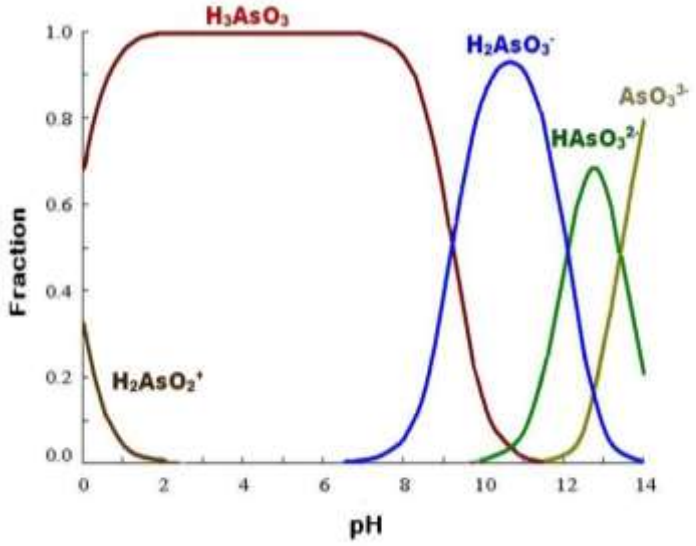

Figure 4. As(III) speciation diagram as a function of pH calculated for an aqueous sodium arsenite with initial concentration of 50 mg/L.

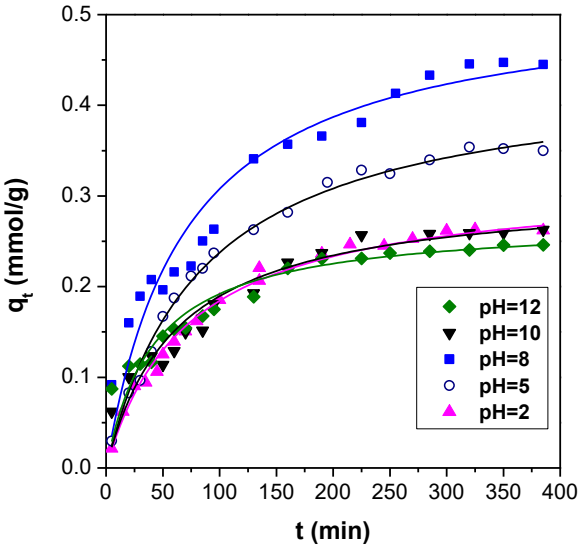

Figure 5. (a) Temporal evolution of the As(III) amount adsorbed on SBA15-SH-40 as a function of solution pH. Solid lines were obtained from pseudo-second order kinetics fitting.

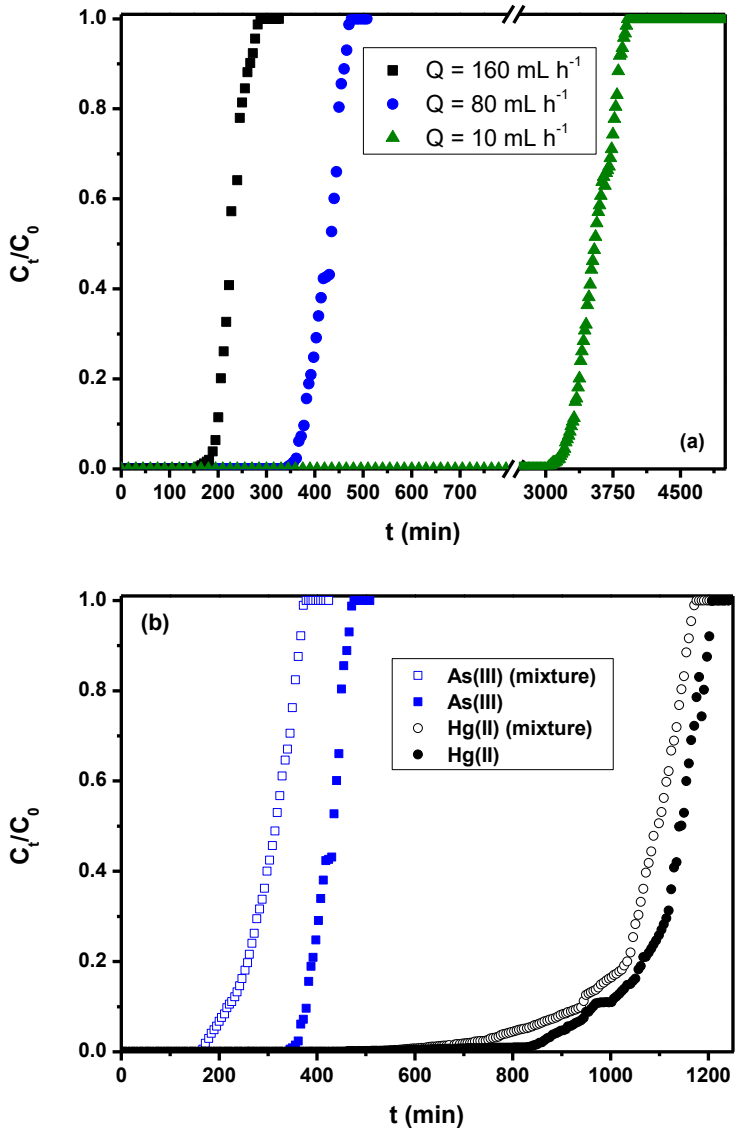

Figure 6. Breakthrough curves from fixed-bed column adsorption experiments on A-SBA15-SH-10 for the initial concentration C_0 = 0.05 mmol L^{-1}. (a) As(III) adsorption as a function of the volumetric flow rate. (b) Competing adsorption between mercury and arsenic for an equimolar As(III) and Hg(II) mixture at flow rate Q = 80 mL h^{-1}.